Microstructure of Titanium-Cement-Lithium Disilicate Interface in CAD-CAM Dental Implant Crowns: A Three-Dimensional Profilometric Analysis

Stefano Cresti, MSc;* Angelo Itri, MD, DDS;† Alberto Rebaudi, MD, DDS;‡ Alberto Diaspro, PhD;§ Marco Salerno, PhD¶

ABSTRACT

Background: Peri-implantitis is an infection of the implant surface caused by adhesion of bacteria that generate bone resorption and sometimes even consequent implant loss. Both screw-retained and cemented fixed implants are affected.

Purpose: The purpose of this study is to investigate the morphological defects at the cemented interface between titanium abutment and ceramic crown, comparing different adhesive cements used to fill the marginal gap.

Materials and Methods: Twelve computer-aided design–computer-aided manufacturing dental crowns were cemented to titanium abutments using three different resin composite cements. Sealed margins were polished using grommets with descending diamond particle size. Three groups of four crowns each were made according to the cement used, namely RelyX Unicem (3 M ESPE), Panavia F 2.0 (Kuraray), and NX3 (Nexus Kerr). Samples were analyzed using optical inspection, three-dimensional profilometry, and image analysis, including analysis of variance.

Results: Although RelyX showed significantly lower root mean square surface roughness (4.4 ± 1.5 µm) than that of NX3 (7.0 ± 2.9 µm), it showed no significant difference with Panavia (3.7 ± 1.5 µm). The marginal gap was significantly wider in Panavia (149 ± 108 µm) as compared with NX3 (71 ± 45 µm) and Relyx (64 ± 34 µm). For all groups, homogeneous heights of both metal-cement and ceramic-cement gaps were observed. Moreover, all samples showed homogeneity of the margins and absence of instrumental bias, thus validating both procedure and materials.

Conclusions: When using the chosen polishing method, RelyX Unicem showed both low roughness and marginal width, and thus the smoothest and more continuous abutment-crown interlayer, promising a low probability of occurrence of peri-implantitis.

KEY WORDS: CAD-CAM, CEREC, dental implants, marginal gap, stylus profilometer, surface roughness

INTRODUCTION

Oral implantology is the branch of dentistry that allows for the rehabilitation of the odontostomatognatic system by means of surgical and prosthetic techniques suitable for the insertion of dental implants. To restore the lost elements, a dental implant must be connected with an abutment for which the prosthetic device will be designed and manufactured. The long-term success of a dental implant is determined by several biological factors, such as osseointegration[1–3] and the quantity/quality of keratinized mucosa that surrounds the prosthetic body,[4–6] as well as the mechanical properties of the prosthesis.[7,8]

*MSc student, University of Genova, Genova, Italy; †private practice, Dental Offices of Rebaudi & Associates, Genova, Italy; active member, Biomaterials Clinical Research Association, Pescara, Italy; ‡private practice, Dental Offices of Rebaudi & Associates, Genova, Italy, and assistant professor, University of Genoa, Genoa, Italy; secretary, Biomaterials Clinical Research Association, Pescara, Italy; §associate professor, University of Genova, Genova, Italy, and director, Nanophysics Department, Italian Institute of Technology, Genova, Italy; ¶research technologist, Nanophysics Department, Italian Institute of Technology, Genova, Italy

Reprint requests: Mr. Stefano Cresti, via Atto Vannucci 9/7, Genova, I-16128 Italy; e-mail: stefano.cresti@hotmail.it

DOI 10.1111/cid.12133

The implant pathology most studied in recent decades is peri-implantitis,[9,10] an infection of the implant surfaces caused by the adhesion of various bacterial species that generate peri-implant bone resorption and consequent loss of the implant itself.[11,12] One key point for long-term maintenance of an implant is the capability of the patient to remove the bacterial biofilm from the prosthetic components.[13,14] To achieve this goal, the use of implant designs and materials that do not allow easy coupling of the biofilm is paramount. In this regard, both screw-retained and cemented fixed implant prostheses are employed. The range of types of cemented prosthesis has been expanded in recent years by means of both novel materials and techniques. In particular, with the introduction of computer-aided design–computer-aided manufacturing (CAD-CAM) equipment, dentists have begun to fabricate chairside inlays, bridges, and crowns, along with preparation of the tooth. Nonetheless, the need to passivate the tensions caused by chairside cementation or screwing of structures is very important in order to reduce bone trauma and prosthetic fractures, especially when an immediate load is applied.[15–17]

One of the ceramic materials most recently studied is lithium disilicate, a glass-ceramic material that reaches a compressive strength of about 360 MPa after a special cooking cycle. Lithium disilicate can be used in the laboratory by means of a wax loss pressing process[18] and in the dental office by milling monolithic parallelepipeds using a milling unit that exploits a CAD-CAM technology.

In the present study, we took advantage of the CAD-CAM chairside technology, and fixed prosthesis was realized and cemented onto standard implant abutments that were then screwed to the implant inserted in the bone.[17] This type of prosthesis requires the construction of a ceramic crown with a passing hole that allows access to the implant-abutment fixing screw. Moreover, the prosthesis can be removed and finished after chairside passive cementation before final fixation with a passing screw. As such, this procedure allows for better removal of the cement from the margins of the abutment and better control of polishing at the abutment–crown-cement double interface.[17] To successfully implement these devices, it is critically important to identify the type of cement presenting the best finished surface, but also having high mechanical adhesion and long-term stability in contact with oral fluids. Whereas different types of cements exist such as zinc phosphate and glass ionomers, in this work, we restricted our scope to one type of cements only, namely the resin composites cements. Therefore, the aim of this study was to investigate the degree of morphological defects at the interface between implant screw and crown when using three different resinous cements to seal the margin in CAD-CAM screwed prosthesis.

MATERIAL AND METHODS

Twelve CAD-CAM dental implant crowns were divided equally into three groups according to the cement used, including RelyX Unicem by 3 M ESPE (hereinafter termed Rel; 3M ESPE, Seefeld, Germany), Panavia F2.0 by Kuraray (hereinafter termed Pan; Kuraray, Hattersheim am Main, Germany), and NX3 by Nexus Kerr (hereinafter termed NX3; Kerr, Orange, CA, USA). Every crown was manufactured at the dental offices of Dr. Alberto Rebaudi (http://www.promogenova.it/studio-rebaudi/index.php) by Dr. Angelo Itri. The samples were analyzed at the Italian Institute of Technology (http://www.iit.it) under the direction of Dr. Marco Salerno.

Each sample is composed of a standard conical titanium abutment (7 mm high with shoulder height at 90° and width of 2 mm) and a CAD-CAM lithium disilicate crown of the tooth fitting the corresponding position on the bone-gingiva model. The abutment (Ti-Bone, Basel, Switzerland) is sprayed with BlocTalk (VITA, Bad Säckingen, Germany) before scanning. The three-dimensional tooth models are made using the CEREC 3D (Sirona Dental Systems, Bensheim, Germany) software and milled out of IPS e.max CAD size C14 glass-ceramic blocks (Ivoclar Vivadent, Bolzano, Italy) using a CEREC MC XL milling unit (Sirona Dental Systems). After a dedicated cooking cycle according to the manufacturer's instructions, every crown is treated in successive ultrasonic cleansing baths: 5 minutes in distilled water, 10 minutes in ultrapure ethyl alcohol for degreasing, 5 minutes in distilled water, and, finally, 1 minute in 9.7vol% hydrofluoric acid gel. Afterwards, in order to improve adhesion to the particular cement used, a Clearfil™ ceramic primer (Kuraray) is applied to the crown surface, according to the instructions of the respective manufacturer (Figure 1). The polishing technique chosen for the samples of this study consists of three rotating grommets with descending diamond particle size. We think that such a sequence can best treat materials having different physical characteristics.

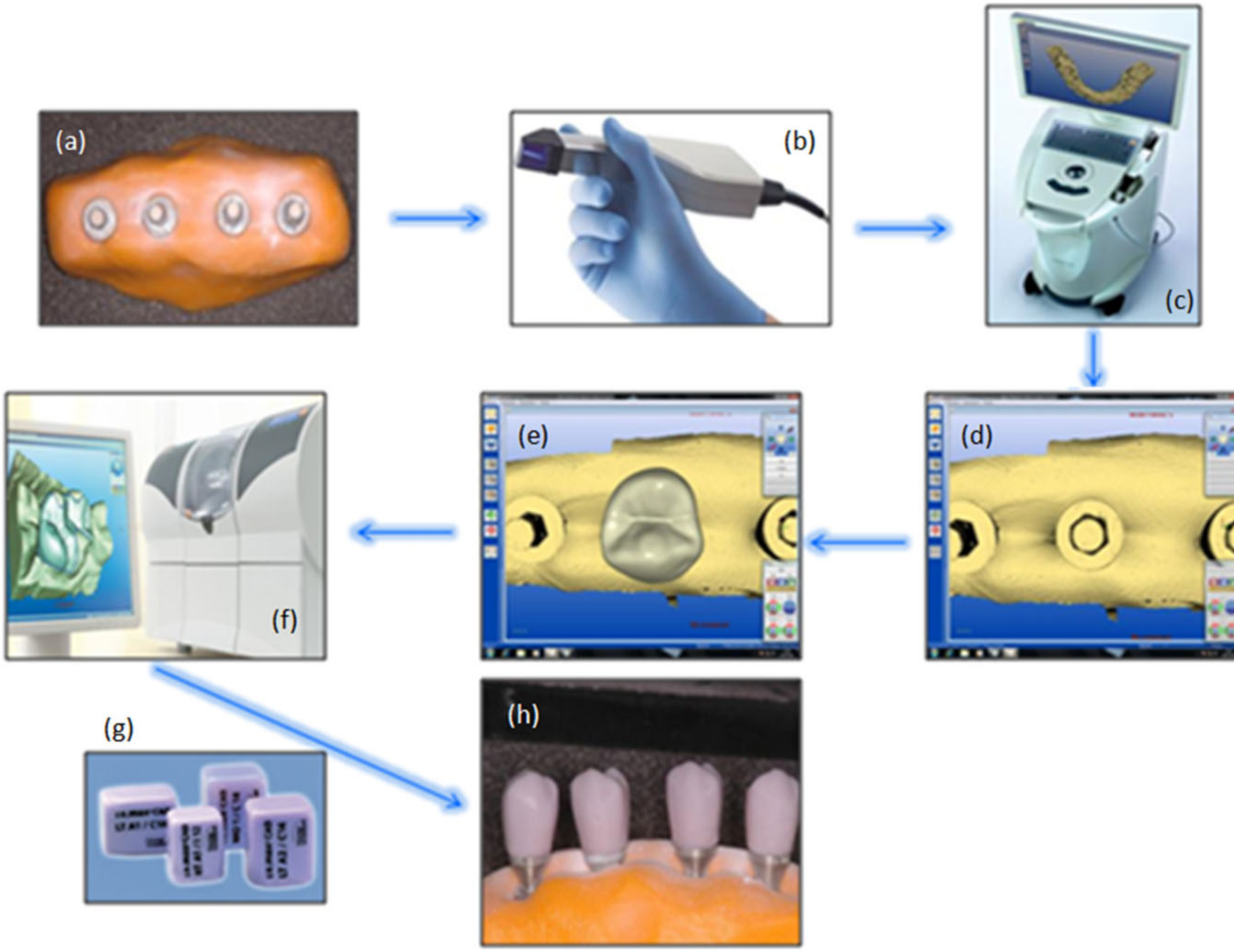

Figure 1 Sample design and manufacturing procedure. After (A) mounting the four titanium abutments ex situ onto the model of patient's bone gingiva to be treated, the model is scanned with an optical pen (B) connected to a digital camera. The computer processing unit then (C) generates a three-dimensional reconstruction (D) on which appropriately shaped teeth (E) are fit. These data are then sent to the milling machine (F), in which the disilicate cubes (G) are loaded, finally resulting in the crowns assembled on the implants (H).

Implant Analysis

The analysis of the realized implants consisted of three phases: morphological reconstruction of the three-dimensional sample surfaces, image analysis, and statistical analysis of the extracted data.

Morphological Reconstruction

Before measurements were taken, an optical inspection of the specimens was performed under a stereomicroscope (EZ4D; Leica Microsystems, Wetzlar, Germany) at 8× to 35× magnification. For each implant, four regions were selected for subsequent topographical measurement by rotating the implant approximately 90° around the axis of symmetry of the fixture between different positions. Each region was then imaged both in side view (Figure 2a) to determine the step-height at the marginal gap and in top view (Figure 2b). The region of interest is the strip of cement at the interface between the metal on one side and ceramic on the opposite side (left and right in Figure 2a and b, respectively). In order to better identify the cement interlayer under the optical microscope, the region of metal-ceramic interface was marked with an indelible red ink pen. This increased the optical contrast of cement owing to the higher roughness and permeability of this material, which captures the color better than the material of the other two surrounding surfaces.

Next to the cemented region, approximately 0.5 mm away from its interface to the abutment, a mark was made by indenting the metal manually with a tungsten

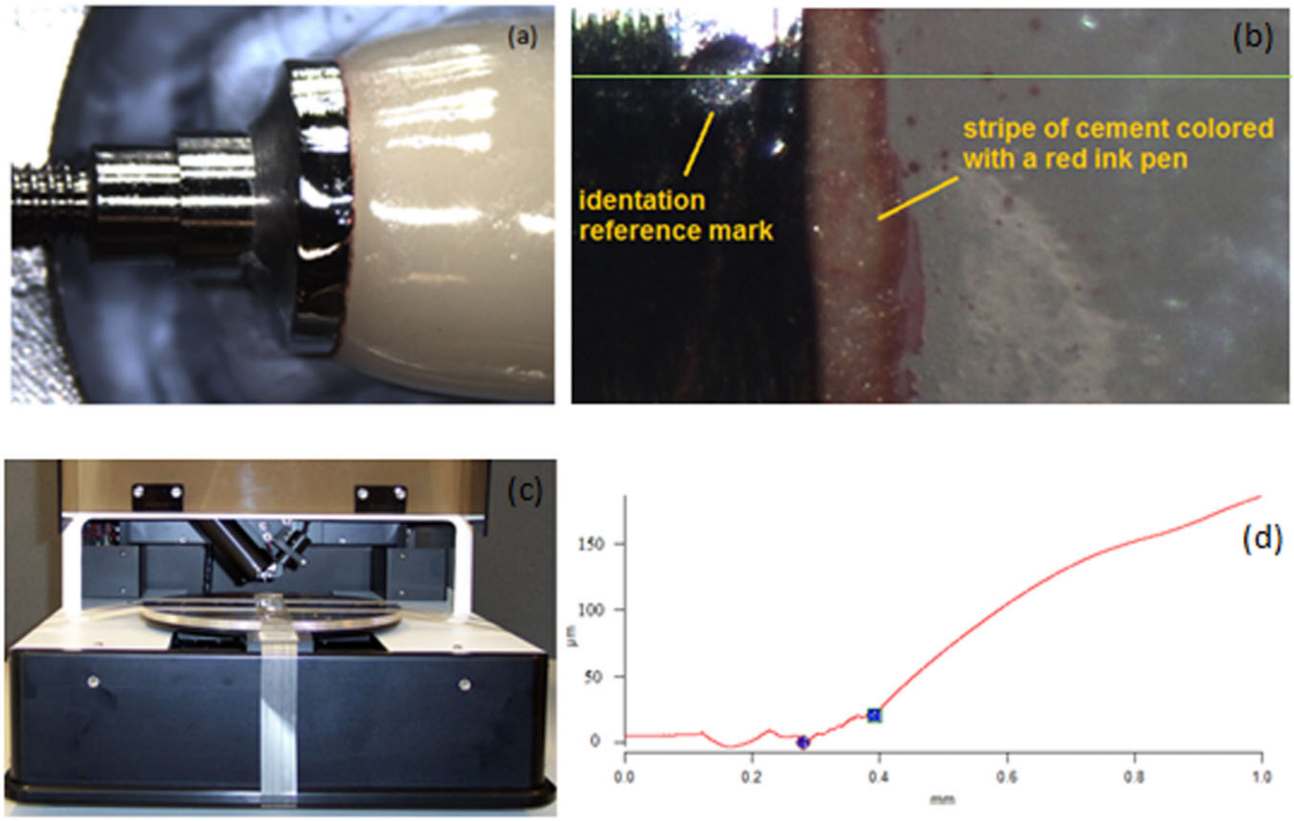

Figure 2 *A* and *B*, Digital images of a typical implant by stereomicroscope, including (A) side view (8× magnification) and (B) top view details (35× magnification) of the handmade scriber indentation on the height profile. *C*, The profilometer used in this study to obtain topographic profiles as in (D), as measured across the position marked by the horizontal green line overlaid on the optical image in (B).

carbide scriber. Using this scriber mark as a reference, a topographical structure could be made for the subsequent topographical analysis.

The specimens were mounted in the XP-2 Profilometer (Ambios Technology, Santa Cruz, CA, USA; see Figure 2c) with the aid of a plasticine bead. A diamond tip with nominal radius of curvature of ~1 µm was used to contact and scan the specimen surface. The profilometer measures precision step-heights and surface roughness as small as 1 nm and as large as 100 µm, providing five orders of magnitude of precision z height measurement, giving height profiles similar to the one in Figure 2d. During the scan, the lateral position of the specimen was set such that the reference indentation previously made by tungsten carbide scriber would permit identification of the position of the metal-cement interface across the acquired profile by assigning the same in-plane distance from the marker as that previously observed in the top view stereomicroscope image (Figure 2b). Initially, a single scan line (in direction x, "fast axis") of fixed length (1 mm) was made with a sampling of 1,618 data points until the mark could be properly captured. Subsequently, a series of 100 lines spaced at intervals of 5 µm was automatically acquired from an initial transverse position shifted away by approximately 250 µm (e.g., half the extension of the area to be covered), and the scan of the "slow axis" y was begun in the opposite direction. Finally, the multiple scan of the 100 profiles was reassembled into a three-dimensional image with the aid of a suitable routine made in Igor 6.22 (Wavemetrics, Portland, OR, USA), and the result is similar to that shown in Figure 3a. The limitation of transversal line displacement of 5 µm results from the limited accuracy of the profilometer in this direction. Consequently, the reconstructed images have an aspect width : height ratio of 2:1, with rectangular pixels of 0.618 µm × 5 µm (e.g., elongated along the y axis by a factor ~8). Despite these limitations, the ±2.5 µm accuracy in the position of the height measurements is still much lower than the typical margin width (50–100 µm) and thus sufficiently precise for proper mapping.

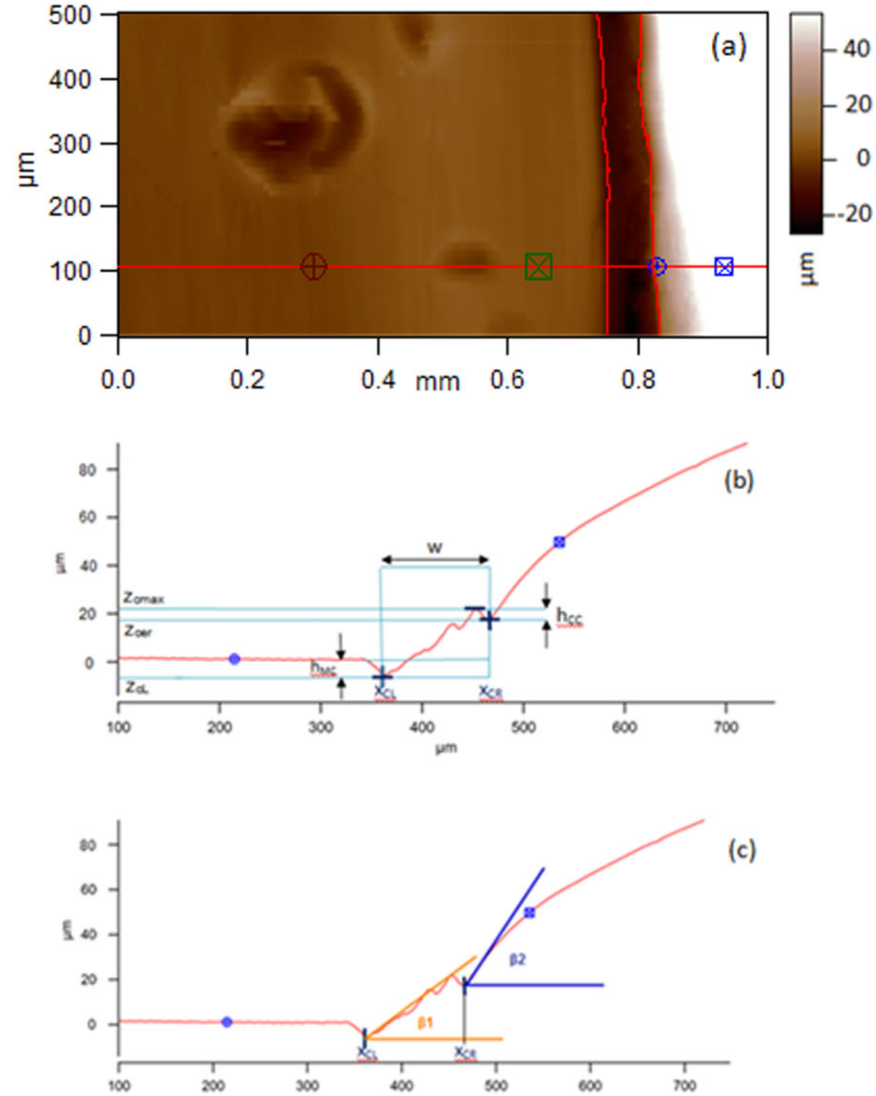

Figure 3 *A*, Typical 2D reconstructed topographical image and (B, C) profile section at the position represented by the red line in (A). For (B) and (C), the parameters are defined as follows: *B*, the three 1D parameters measured include w, h_{mc}, and h_{cc}; and *C*, two 2D parameters, β1 and β2. From (A) the other 2D parameter, namely, surface roughness Sq restricted to the cement interlayer region is obtained.

Image Analysis

Sixteen images each were obtained for the three cement groups for a total of 48 images. From each image, four representative lines among the 100 available profiles were chosen. In the case of regions with variant characteristic behavior within a given image, the profiles were selected to be representative of these different local behaviors. Conversely, in the case of apparently uniform images, equally spaced lines at positions numbered 20, 40, 60, and 80 were selected by convention. This protocol was necessary to ensure that the results would have statistical significance for the 1D parameters extracted from individual profiles. Prior to analysis, the 2D planar background of the surface was removed in the region of the metal to make it the reference region with horizontal cross section corresponding to the x-axis (e.g., $z = 0$) in Figure 3.

Figure 3b graphically shows the following 1D morphological parameters calculated for each profile:

- The width of the cement interlayer w, defined as the x distance on the horizontal axis between the cement margin positions (index c), respectively, on the left and on the right image side (e.g., $w = X_{cR} - X_{cL}$);
- The height of the step between level z of the flat horizontal metal area far away from the cement

(e.g., $z = 0$) and level z of the metal interface with the cement or Z_{CL} (e.g., $h_{mc} = Z_{cL}$);

- The height of the step between the cement and ceramic or $h_{cc} = Z_{cmax} - Z_{cer}$.

In order to help identify the cement edges on the assembled image away from the indentation reference mark, we used a 3×3 kernel filter available in the software, based on a Sobel differential operator,[19] which allows for recognition of contours of regions with different local surface gradient. This filter is useful because it allows the slopes on the three-dimensional images to be easily visualized and also shows different lateral patterns (graininess) on the cement in contrast to the smoother metal and ceramic surfaces.

For each image, three other parameters were also calculated, representing a mean property of the whole image and thus called 2D parameters:

- The surface roughness of the cement S_q is calculated as the root mean square (RMS) of the area associated with this region, after appropriate masking with the help of the above-mentioned gradient-based filter.
- The absolute value β_1 of the angle formed by the intersection of the plane which best approximates the cement region with the horizontal plane parallel to the x axis;
- The angle β_2 formed by the intersection of the plane which best approximates the crown region closest to the cement with the horizontal plane parallel to the x axis.

Originally, as graphically described in Figure 3c, β_1 and β_2 are both 1D parameters but they have been averaged through all 100 profiles in an image, thus gaining 2D character.

To calculate the three 2D parameters S_q, β_1, and β_2, it was necessary to create a mask limiting the surface portion of the image representing the region of interest (e.g., the cement region for β_1 and S_q, and the crown region for β_2). This mask was obtained by manual drawing of elementary CAD regions of interest in the shape of rectangles and ellipses.[19]

Statistical Analysis

In total, for each crown, the 1D parameters were assigned a number of different values of $N_{1D} = 4 \times 4 = 16$. In contrast, for the 2D parameters, the statistic is more limited as only a single parameter value is extracted from each image (e.g., $N_{2D} = 4$). For each parameter, an analysis of variance (ANOVA) was performed, with Tukey test at three levels of significance starting from $\alpha = 0.05$ and proceeding at progressively more restrictive levels of $\alpha = 0.01$ and possibly $\alpha = 0.001$. Tukey is one of the tests most used in ANOVA for comparisons between pairs of groups to assess the statistical significance of their different values.

RESULTS

Means and standard deviations were calculated for a total of 4 crowns/cement × 4 images/crown = 16 images for 2D parameters S_q, β_1, and β_2, and for 4 crowns/cement × 4 images/crown × 4 profiles/image = 64 profiles for the 1D parameters. The overall results for the three types of cements considered are reported numerically and graphically in Table 1 and in Figure 4, respectively. The error bars in the plot of Figure 4 have size equal to one standard deviation ($\pm 1\ \sigma$).

We tentatively define here the fit at the abutment-crown interface as excellent when the following constraints on the above parameters are satisfied: S_q <5 μm and w ≤100 μm, and all the other quantities as low as possible (e.g., h_{mc} ≤15 μm, h_{cc} ≤5 μm, $\beta_1 \leq 15°$, and $\beta_2 \leq 40°$). In this respect, all cements seem to exhibit good fit.

The graph in Figure 5a (black columns in Figure 4) shows that Rel presents surface roughness S_q similar to that of Pan (4.4 ± 1.5 μm and 3.7 ± 1.5 μm, respectively) but lower than that of NX3 (7.0 ± 2.9 μm). At the

TABLE 1 Means and Standard Deviations of the Measurements of All Parameters for the Three Cements

Cement	$S_q \pm \Delta S_q$ (μm)	$w \pm \Delta w$ (μm)	$h_{mc} \pm \Delta h_{mc}$ (μm)	$h_{cc} \pm \Delta h_{cc}$ (μm)	$\beta_1 \pm \Delta\beta_1$ (°)	$\beta_2 \pm \Delta\beta_2$ (°)
Rel	4.4 ± 1.5	64 ± 34	15.1 ± 9.1	3.0 ± 6.2	10.9 ± 9.5	34.5 ± 16.8
Pan	3.7 ± 1.5	149 ± 108	20.7 ± 19.3	2.1 ± 4.9	10.2 ± 5.2	45.4 ± 15.4
NX3	7.0 ± 2.9	71 ± 45	21.5 ± 18.0	6.0 ± 9.8	15.1 ± 8.4	41.6 ± 15.5

Rel, RelyX Unicem; Pan, Panavia F2.0.

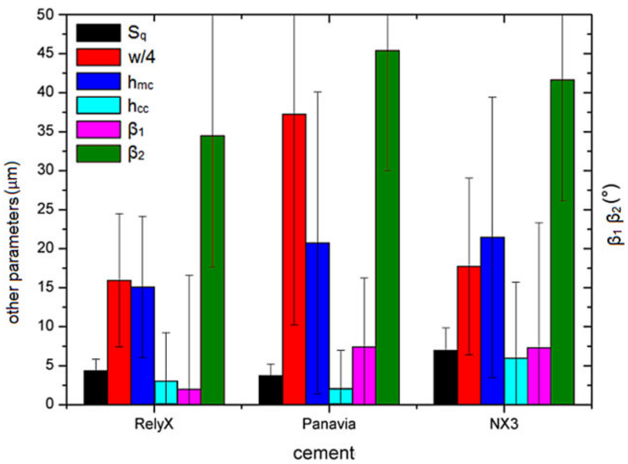

Figure 4 Graphical representation of means and standard deviations of the measurements of all parameters for the three cements. The error bars are ±1σ centered around the mean.

significance level $\alpha = 0.01$, the differences between NX3 and the other two cements are both confirmed, whereas at the most restrictive significance level ($\alpha = 0.001$), the difference between NX3 and Rel, disappears, and only the difference between NX3 and Pan remains.

The space w filled by the cement between the titanium shoulder of the abutment and the closing edge of the crown, for example, the marginal gap (Figure 5b and red columns in Figure 4), is significantly larger ($\alpha = 0.05$) in the samples cemented with Pan (149 ± 108 µm) compared with NX3 (71 ± 45 µm) and Rel (64 ± 34 µm). This difference remains valid in both cases also at the higher significance levels.

Regarding the metal-cement step height h_{mc} (Figure 5c and blue columns in Figure 4), despite a lower average level for Rel, all the samples are statistically equivalent to each other and thus without statistical difference, even at the lowest level of significance of $\alpha = 0.05$.

For the step height between cement and ceramic h_{cc} (Figure 5d and cyan columns in Figure 4), a statistically significant difference ($\alpha = 0.05$) only appears between NX3 and Pan, whereas, despite the higher average, h_{cc} of NX3 is not significantly greater than that of Rel. The difference between NX3 and Pan remains at the significance level of $\alpha = 0.01$, only disappearing at $\alpha = 0.001$.

For the 2D parameter β_1 (Figure 5e and magenta columns in Figure 4), despite a higher average level for NX3, all the samples are statistically equivalent at the already milder level of significant difference, $\alpha = 0.05$. The same also holds true for β_2 (Figure 5f and green columns in Figure 4).

DISCUSSION

From the point of view of bone osteointegration, possible micromotion occurring during the healing phase is the most important factor, which is probably affected by the misfit at the abutment-implant interface. Nevertheless, a misfit at the abutment-crown interface is probably more important for the tissues in the long run, and in this investigation, we have focused on the work done by the dentist when treating this misfit.

The first parameter normally considered when evaluating the finishing of a dental surface is roughness. Clearly, low roughness is desired on all dental surfaces as this minimizes the rate of bacterial adhesion, forming biofilm and initiating plaque and eventually caries.[20–23] Whereas for single dental material surfaces, the golden standard for evaluation of roughness is the atomic force microscope;[20,24] for complex systems such as the present three-materials interface, the large inspection volume required makes it necessary to use the three-dimensional profilometry developed here. According to the literature, the best system for polishing the edge of the crown in lithium disilicate is the sequence characterized by three finishing discs,[25] whereas no consensus has been reached on the best system for finishing the cement layer. In this work, we analyzed the performance of the polishing technique chosen here by the analysis of different surface parameters.

Looking at the RMS roughness of the cement layer, the three resinous compounds investigated here all exhibit a similar behavior after polishing. Regarding the 2D parameters derived from surface region angles, it should be noted that angle β_2 between crown and horizontal implant axis is always positive (e.g., pointing upwards from left to right) but the angle formed by the cement can be negative (e.g., pointing downward locally) in some cases of imperfect cement removal by the polishing procedure. In fact, a slightly increasing upward direction would allow for a smoother connection to the ceramic, at least from a geometric point of view. However, this would, in turn, result in an increase of the extension w of the cement region, which is generally undesired, particularly because the typically greater roughness of the cement region could have pathological consequences of the type noted above (e.g., peri-implantitis).

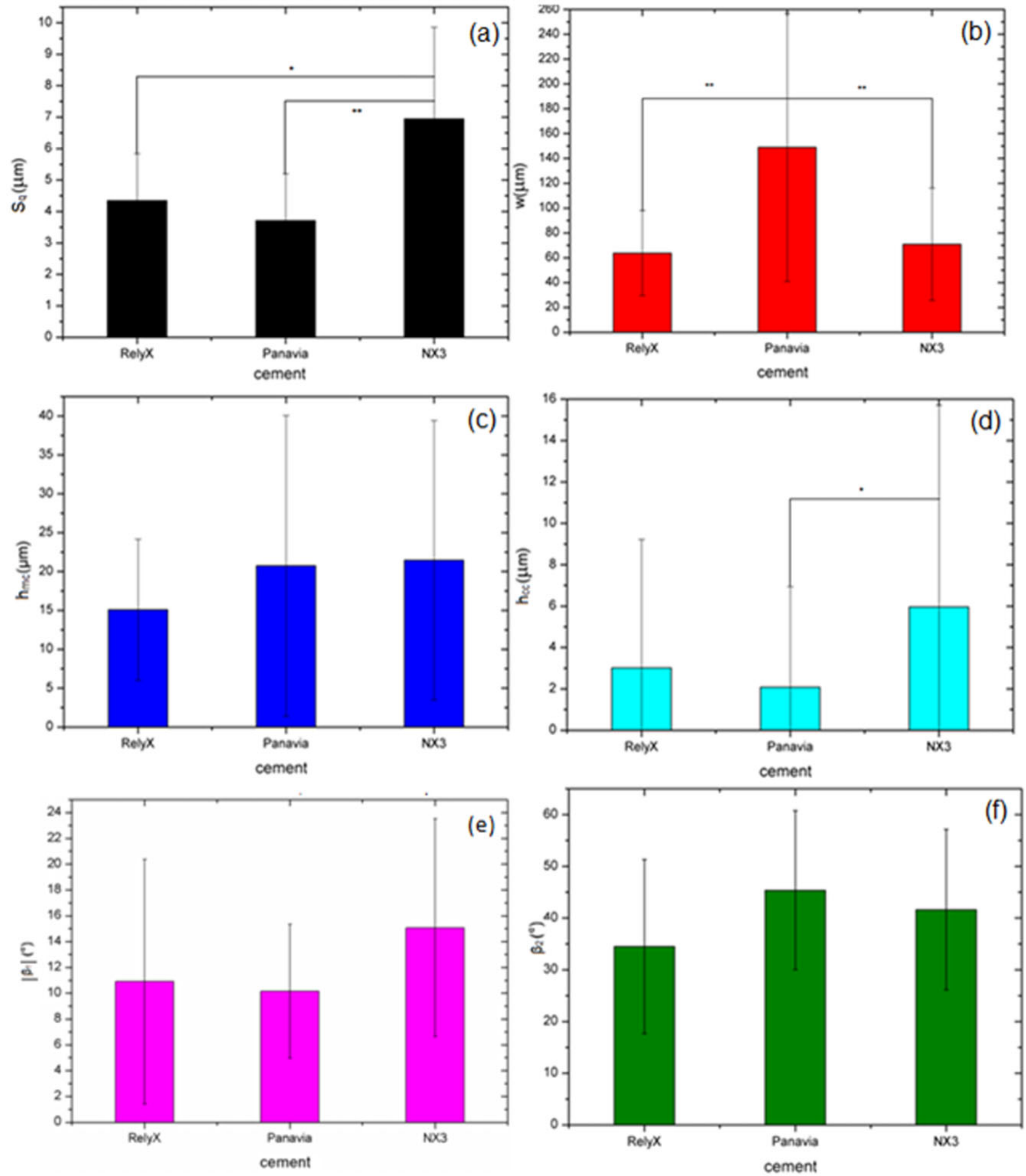

Figure 5 Detailed views of the comparisons for each morphological parameter among the different cements, with respective considerations on the statistical significance (in case of positive differences found: *$\alpha = 0.01$, **$\alpha = 0.001$).

Reviewing the results in Table 1 and Figures 4 and 5, it can be seen that the group Rel specimens presented surface roughness equivalent to that of specimens in group Pan, but lower than that of specimens in group NX3. In the literature, some authors have tested the degree of morphological defects in CAD-CAM crowns after polishing was carried out with different techniques,[25–27] whereas other authors have evaluated the surface roughness of glass ionomer and resinous cements[21,28,29] with profilometer after polishing by means of various techniques. None of these studies included a type of prosthesis similar to the one carried out for this analysis. In fact, these studies evaluated the cement finishing of samples in the form of discs[22,23] or on teeth extracted and prepared with standard procedures.

ANOVA showed that the marginal gap width was significantly higher in the specimens cemented with Pan compared with NX3 and Rel, and that this difference remained valid for all three significance levels. This result suggests a higher difficulty in the manipulation of Pan than Rel or NX3 based on its high mechanical characteristics of resistance to compression that make the finishing with the sequence of the three rubbers more laborious[30,31] (Kuraray Medical Inc., http://www.panavia-dental.eu).

CONCLUSION

Within the limitations of this in vitro study, the following conclusions can be drawn:

- The finishing of the closing edge of screw-retained prosthesis presents similar difficulties as for cemented prosthesis, such as difference in hardness and abrasion resistance of the abutment titanium, the cement interlayer, and the crown lithium silicate.
- The resin cements used are all able to fill the gap between disilicate crown and titanium abutment properly after polishing. This is consistent with clinical practice where screw-retained crowns seem to permit a better finishing as compared with cemented ones, because margins can be polished after removing the crown under microscopic control, whereas with cemented crowns the polishing must be performed at chairside, causing difficulty in margins close to adjacent teeth.
- Although all the cements tested gave acceptable finishing with the chosen polishing method, Rel had the best performance in providing a smooth and continuous cement abutment–crown interlayer, as it provided simultaneously the lowest RMS level – similar to Pan and lower than NX3 – and the lowest marginal gap – similar to NX3 and lower than Pan. The homogeneity of sample design and the absence of instrumental bias, which validate the analysis, were guaranteed by the processing being done by a skilled user.
- Because all the tests presented here were performed in vitro, it would be interesting in the future to evaluate the levels of polishing and fit that can be obtained in vivo after polishing at chairside comparing screw-retained with cemented restorations.

REFERENCES

1. Brånemark PI. Osseointegration and its experimental background. J Prosthet Dent 1983; 50:399–410.
2. Anneroth G, Hedström KG, Kjellman O, Köndell PA, Nordenram A. Endosseus titanium implants in extraction sockets. An experimental study in monkeys. Int J Oral Surg 1985; 14:50–54.
3. Linkow LI, Rinaldi AW. The significance of fibro-osseous integration and osseointegration in endosseous dental implants. Int J Oral Implantol 1987; 4:41–46.
4. Etter TH, Håkanson I, Lang NP, Trejo PM, Caffesse RG. Healing after standardized clinical probing of the perlimplant soft tissue seal: a histomorphometric study in dogs. Clin Oral Implants Res 2002; 13:571–580.
5. Yeung SC. Biological basis for soft tissue management in implant dentistry. Aust Dent J 2008; 53(Suppl 1):S39–S42.
6. Tözüm TF, Güncü GN, Yamalik N, Turkyilmaz I, Güncü MB. The impact of prosthetic design on the stability, marginal bone loss, peri-implant sulcus fluid volume, and nitric oxide metabolism of conventionally loaded endosseous dental implants: a 12-month clinical study. J Periodontol 2008; 79:55–63.
7. Papaspyridakos P, Chen CJ, Singh M, Weber HP, Gallucci GO. Success criteria in implant dentistry: a systematic review. J Dent Res 2011; 91:242–248.
8. Law C, Bennani V, Lyons K, Swain M. Mandibular flexure and its significance on implant fixed prostheses: a review. J Prosthodont 2012; 21:219–224.
9. Zitzmann NU, Berglundh T. Definition and prevalence of peri-implant diseases. J Clin Periodontol 2008; 35:286–291.
10. Huynh-Ba G. Peri-implantitis: “Tsunami” or marginal problem? Int J Oral Max Impl 2013; 28:333–337.
11. Esposito M, Hirsch JM, Lekholm U, Thomsen P. Biological factors contributing to failures of osseointegrated oral implants (II). Etiopathogenesis. Eur J Oral Sci 1998; 106: 721–764.
12. Romeo E, Ghisolfi M, Carmagnola D. Peri-implant diseases. A systematic review of the literature. Minerva Stomatol 2004; 53:215–230.
13. Serino G, Ström C. Peri-implantitis in partially edentulous patients: association with inadequate plaque control. Clin Oral Implants Res 2008; 20:169–174.
14. Persson GR, Samuelsson E, Lindahl C, Renvert S. Mechanical non-surgical treatment of peri-implantitis: a single-blinded randomized longitudinal clinical study. II. Microbiological results. J Clin Periodontol 2010; 37:563–573.

15. Karl M, Winter W, Taylor TD, Heckmann SM. In vitro study on passive fit in implant-supported 5-unit fixed partial dentures. Int J Oral Maxillofac Implants 2004; 19:30–37.
16. Rebaudi A, Pascetta R, Rebaudi O, Rebaudi F. Presurgical implant-supported prosthesis: technique for cementation of a definitive prosthesis immediately after surgery. Int J Periodont Restor Dent 2006; 26:439–451.
17. Rebaudi A. The ray setting procedure: a new method for implant planning and immediate prosthesis delivery. Int J Periodont Restor Dent 2007; 27:267–275.
18. Culp L, McLaren E. Lithium Disilicate: the restorative material of multiple options. Compendium 2010; 31:716–725.
19. Russ John C. The image processing handbook. 6th ed. Boca Raton, FL: CRC Press, 2011.
20. Salerno M, Giacomelli L, Derchi G, Patra N, Diaspro A. Atomic force microscopy in vitro study of surface roughness and fractal character of a dental restoration composite after air-polishing. Biomed Eng Online 2010; 9:59–69.
21. Bala O, Arisu HD, Yikilgan I, Arslan S, Gullu A. Evaluation of surface roughness and hardness of different glass ionomer cements. Eur J Dent 2012; 6:79–86.
22. Jefferies SR, Boston DW. Conventional polishing techniques versus a nanofilled surface sealer: preliminary findings regarding surface roughness changes and analysis. J Clin Dent 2010; 21:20–23.
23. Ozel E, Korkmaz Y, Attar N, Karabulut E. Effect of one-step polishing systems on surface roughness of different flowable restorative materials. Dent Mater J 2008; 27:755–764.
24. Salerno M, Patra N, Derchi G, Diaspro A. Combined effect of polishing on surface morphology and elastic properties of a commercial dental restorative resin composite. Sci Adv Mater 2012; 4:126–134.
25. Al-Shammery HA, Bubb NL, Youngson CC, Fasbinder DJ, Wood DJ. The use of confocal microscopy to assess surface roughness of two milled CAD-CAM ceramics following two polishing techniques. Dent Mater 2006; 23:736–741.
26. Flury S, Lussi A, Zimmerli B. Performance of different polishing techniques for direct CAD/CAM ceramic restorations. Oper Dent 2010; 35:470–481.
27. Karan S, Toroglu MS. Porcelain refinishing with two different polishing systems after orthodontic debonding. Angle Orthod 2008; 78:947–953.
28. Tarica DY, Alvarado VM, Truong ST. Survey of United States dental schools on cementation protocols for implant crown restorations. J Prosthet Dent 2010; 103:68–79.
29. Abou-Madina MM, Özcan M, Abdelaziz KM. Influence of resin cements and aging on the fracture resistance of IPS e.max press posterior crowns. Int J Prosthodont 2012; 25:33–35.
30. Luthy H, Loeffel O, Hammerle C. Effect of thermocycling on bond strength of luting cements to zirconia ceramic. Dent Mater 2006; 2:195–200.
31. Goracci C, Cury AH, Cantoro A, Papacchini F, Tay FR, Ferrari M. Microtensile bond strength and interfacial properties of self-etching and self-adhesive resin cements used to lute composite onlays under different seating forces. J Adhes Dent 2006; 8:327–335.